Network Stretching during Tensile Drawing of Polyethylene: A Study Using X-ray Scattering and Microscopy

K. Hong* and G. Strobl

Physikalisches Institut, Albert-Ludwigs-Universität, 79104 Freiburg, Germany

Received August 3, 2005; Revised Manuscript Received August 4, 2005

ABSTRACT: Because of the limitation that many semicrystalline polymers are not transparent, one cannot always study the network stress by optical methods. We suggest to use another tool in such a case. By measuring the azimuthal intensity distribution of the amorphous halo with wide-angle X-ray scattering experiments, one can determine the amorphous chain orientation induced in the strained network, which then results in the network stress. Experiments were carried out for a low-crystallinity polyethylene. They yield the relationships between the orientational order parameter associated with the halo, the birefringence produced by the amorphous chain parts, and the stress. The X-ray scattering results also show that the orientation of the amorphous segments under uniaxial drawing is comparable to the degree of orientation of the crystallites.

1. Introduction

The chains in the amorphous regions of semicrystalline polymers are entangled and form a network which acts together with the skeleton of lamellar crystallites; both together hold the applied force. The thickness of the lamellae is usually in the range of several nanometers, and they are arranged in spherulites with sizes in the micrometer range. The properties of both compounds show up at the measured stress−strain curves.

Figure 1 presents as a typical example true stress−true strain curves of polyethylene and some copolymers with various crystallinity.[1] All of the curves have a common shape. The initial part, which varies with the crystallinity, is determined by the crystal skeleton, and the final part with a constant shape relates to the entanglement network. Stresses at first show a softening and then at higher strains a hardening. The mechanical changes are related to the structural changes. At point B a cooperative sliding of the crystal blocks composing the lamellae sets in resulting in a plastic deformation of the crystal skeleton. Point C represents a critical strain, at which the crystal blocks begin to be destroyed and a fibrillar structure forms. It was found that for all polyethylenes under study the strains at B and C were constant, with $\epsilon_H(B) \approx 0.1$ and $\epsilon_H(C) \approx 0.6$. The critical strains are also invariant when varying the strain rate and the temperature.[2] On the basis of this fact, the deformation properties have been addressed as being strain controlled.

The stress, as observed in tensile stretching tests, can be considered as being composed of three contributions: (i) the forces transmitted by the skeleton of crystal blocks, σ_c; (ii) the force brought up by the stressed amorphous network, σ_n, and (iii) viscous forces, σ_r, which might come from the sliding between the crystal blocks, from the sliding between polymeric chains, or from the rotation of molecular units.

We applied stress relaxation measurements to separate the viscous stress from the total applied stress.[3] The stress which remains after the subtraction of the viscous stress represents the sum of the network stress and the skeleton stress. A second step in the decomposition was based on the assumption that at high strains one can treat a semicrystalline polymer as a rubberlike amorphous network with crystallites as fillers. Plotting the quasi-static stress vs $\lambda^2 - 1/\lambda$, the measure of strain for a rubber with λ denoting the elongation ratio, the shear modulus of the network could be determined from the asymptotic behavior at large strains.[3]

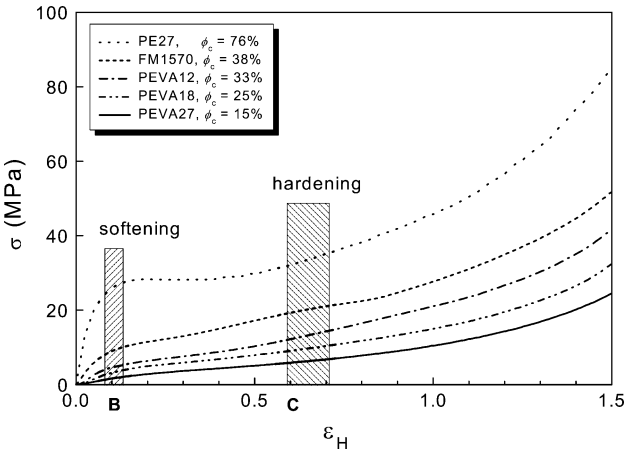

Figure 1. Relation between the true stress and the true strain for the five samples under study, obtained by video-controlled stretching experiments at a constant strain rate $\dot{\epsilon}_H = 0.005\ s^{-1}$. Measurements were carried out over similar ranges, away from the points of fracture (from ref 1).

We also searched for a means to directly measure the network stretching and thus the network stress. As described in this contribution this can be achieved by X-ray scattering experiments. As demonstrated firstly by Pick et al.[4] for a noncrystalline polymer, the orientational order shows up in the intensity distribution of the amorphous halo. We used this approach again for a semicrystalline polyethylene and carried out a comparison with results obtained by birefringence measurements in a polarizing microscope. As it turned out, drawing results in similar degrees of orientation of both crystallites and the amorphous network.

2. Experimental Section

2.1. Sample. The studies were carried out with various polyethylenes (PEs). Materials were supplied by BASF AG, Ludwig-

* Corresponding author. E-mail: hong@physik.uni-freiburg.de.

10.1021/ma051726o CCC: $33.50
Published on Web 12/08/2005

Table 1. Properties of PE Samples under Study; Melting Points and Crystallinities Were Derived from DSC Scans

sample	type	source	melting point (°C)	crystallinity (%)	counit content
PE27	linear polyethylene	Hoechst AG, Frankfurt	138	76	
FM1570	poly(ethylene-*co*-octene)	Dow Chemical Europe	112	38	7.5 wt % of counits
PEVA12	poly(ethylene-*co*-vinylacetate)	Exxon Chemical Europe, Machelen, Belgium	93	33	12 wt % of counits
PEVA18	poly(ethylene-*co*-vinylacetate)	Exxon Chemical Europe, Machelen, Belgium	88	25	18 wt % of counits
PEVA27	poly(ethylene-*co*-vinylacetate)	Exxon Chemical Europe, Machelen, Belgium	52	15	27 wt % of counits

shafen (PE27), Dow Chemical Europe (FM1570), and Exxon Chemical Europe, Inc., Machelen, Belgium (PEVA12, PEVA18, and PEVA27). The samples are listed in Table 1 with some characteristic properties indicated. The crystallinities were derived from the heats of fusion. Samples for the measurements were prepared as follows. From 5 to 8 g of pellets was sandwiched between two Teflon sheets. The sandwich was then placed into a press, heated (polyethylene to 180 °C, poly(ethylene-*co*-octene) and poly(ethylene-*co*-vinyl acetate) to 160 °C), compressed to a sheet form, and maintained at this temperature for ~20 min. The plates of the press were then cooled to room temperature in a slow process. From the resulting polymer sheet samples were stamped out, which had the standard "dog-bone" form. The thickness of the samples was 0.5−0.6 mm.

2.2. Microscope. Using a polarizing microscope with a tilting compensator, one can measure the birefringence. The viewing field is dark when the polarizer and the analyzer have crossed orientations. The sample is then placed between the polarizer and the analyzer so that the stretching direction of the sample is at 45° to the axis of the polarizer. The incident polarized beam of light is split into two beams: one vibrating parallel to the stretching direction and the other perpendicular to the stretching direction. Since the refractive indices parallel and perpendicular to the tensile direction are different, $n_{\|} \neq n_{\perp}$, the beams have different velocities and thus develop an optical path length difference, Γ. It can be easily determined with the aid of a tilting compensator. The birefringent compensator plate is tilted until the object appears dark in the center of the viewing field. The birefringence index of the sample, $\Delta n = n_{\|} - n_{\perp}$, then follows from

$$\Delta n = \Gamma/d \tag{1}$$

where d is the thickness.

The crystallinity of PEVA27 was checked by the DSC tests subsequent to different tensile deformations. The results showed that the crystallinity variations were only small, below 3%, and could be neglected. Thus assuming a constant volume during the stretching, the thickness d was related to the extension ratio λ, by

$$d = \sqrt{\frac{d_0}{\lambda}} \tag{2}$$

where d_0 is the original thickness.

The microscope used in this work was an Ortholux II POL-BK, Leitz AG.

2.3. WAXS. Wide-angle X-ray scattering (WAXS) experiments were carried out in order to determine the azimuthal intensity distributions of both Bragg reflections and the amorphous halo of deformed samples. Employing a Mini-Instron (Rheometric Scientific Mini Mat 2000), samples could be kept under stress during the exposure. We used a rotating Cu anode generator (Fa. Schneider, Offenburg) and registered the scattering intensity distributions with an image plate detector (Fa. Schneider, Offenburg). Scattering diagrams were obtained within minutes.

3. Results

3.1. Degrees of Orientation Determined by WAXS. Based on the regularity in the chemical structure of polyethylenes, an orthorhombic crystal lattice is formed in which the chain has a planar zigzag conformation. During the tensile drawing the crystallites retain to a large part the orthorhombic structure; only at high strains also a monoclinic crystal form develops. With WAXS measurements one can study the orientation of the crystallites in semicrystalline polymers based upon the azimuthal intensity distribution along the scattering circles. The X-ray scattering patterns for the unoriented PEVA27 and for five elongations are presented in Figure 2. Starting in the non-deformed state with the isotropic intensity distribution, the first visible changes in the WAXS pattern occur for $\epsilon_H \approx 0.1-0.2$. Four maxima at oblique angles show up for the 110 reflection. Deforming the sample further to $\epsilon_H > 0.6$, the 110 reflection shows maxima at the equator. It is known since long time that the *c*-axis of the polyethylene crystal is gradually turned into the stretching direction as the polyethylene is elongated.[5] More results are presented in the upper part of Figure 3, which gives the azimuthal scans of the intensity distribution of the 110 reflection. In the plot the diffuse intensity originating from the amorphous parts is subtracted.

An orientational order parameter proposed long ago by Hermanns[6] is often used to express quantitatively the degree of orientation of a set of lattice planes *hkl* in uniaxially oriented samples. It is defined by

$$S_{hkl} = \frac{3\langle \cos^2 \vartheta_{hkl} \rangle - 1}{2} \tag{3}$$

Here the angle ϑ_{hkl} denotes the angle between the stretching direction and the normal vector of the *hkl* lattice plane. The value of the order parameter of the 110 lattice plane, S_{110}, can be derived from the azimuthal intensity distribution function $I(\mu)$ along the respective circle by use of the Polanyi equation[7]

$$\cos \vartheta_{110} = \cos \theta_{110} \cos \mu \tag{4}$$

The equation relates the azimuthal angle μ along the Debye circle to the angle ϑ_{110} between the stretching direction and the normal vector of the 110 lattice plane (θ_{110} denotes the Bragg scattering angle).

The results for the orientational order parameters of the 110 reflection are given in the upper part of Figure 4 as a function of the imposed strain. Note that for a perfect orientation of the lattice plane with its normal in the plane of equator, the orientational order parameter would be $S_{110} = -0.5$. This limiting value was not reached.

Monar and Habenschuss found that for polyethylenes the amorphous halo position shifts to larger scattering angles with decreasing temperature.[8] This temperature dependence indicates that the halo first of all originates from the intermolecular scattering. This was also suggested by other researchers,[9,10] who emphasized that the amorphous halo appears in the range of smaller scattering angles ($2\theta < 20°$ for Cu Kα) where intermolecular scattering is stronger than the intramolecular contributions. Therefore, with WAXS measurements one can study not only the orientation of crystallites but also the orientation of the amorphous chains based on the azimuthal intensity distribution of the halo. In this work we studied the intensity distribution of the halo in the range $2\theta = 19-20°$, which is well away from the 110 reflection. As shown in Figure

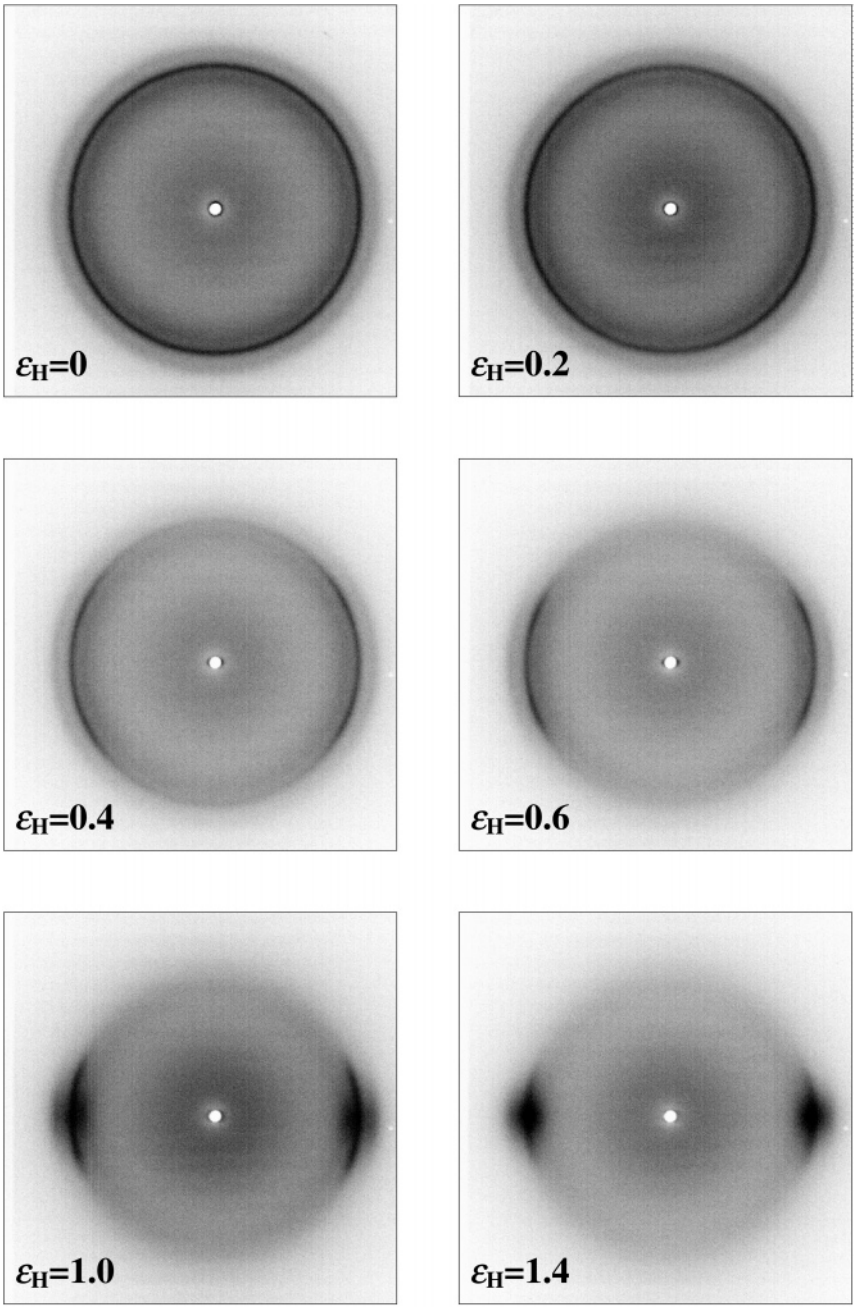

Figure 2. PEVA27: WAXS patterns measured for the indicated strains. The fiber axis is oriented in the vertical direction.

2, the uniaxial elongation of PEVA27 causes the amorphous halo to become anisotropic. Deforming the sample the scattering intensity concentrates more and more on the equator. Detailed results are presented in the lower part of Figure 3, which gives the azimuthal scans of the intensity distribution of the amorphous halo. The background intensity as determined at $2\theta = 15°$ is subtracted.

Again Hermanns' orientational order parameter can be used to express the degree of orientation, now referring to the halo. Denoting it S_{halo}, it follows as

$$S_{halo} = \frac{3\langle \cos^2 \vartheta_{halo} \rangle - 1}{2} \quad (5)$$

where ϑ_{halo} describes the angle between the stretching direction and a vector perpendicular to the local direction of the amorphous chain. The values for S_{halo} can be again derived from the azimuthal intensity distribution function $I(\mu)$ by use of the Polanyi equation[7]

$$\cos \vartheta_{halo} = \cos \theta_{halo} \cos \mu \quad (6)$$

The angle θ_{halo} now denotes the Bragg scattering angle of the halo. The results obtained for the order parameter of the halo are given in the lower part of Figure 4 as a function of the imposed strains. When the amorphous chains would be fully aligned, the order parameter would be $S_{halo} = -0.5$.

Figure 5 presents the orientational order parameter of the halo as a function of strain for the three samples PE27, PEVA12, and PEVA27. The curves of all samples agree with each other. Hence, the imposed strain is taken up by the amorphous parts in equal manner, independent of the crystallinity.

3.2. Comparison with Birefringence Measurements. Semi-transparent PEVA27 pieces were uniaxially stretched under a

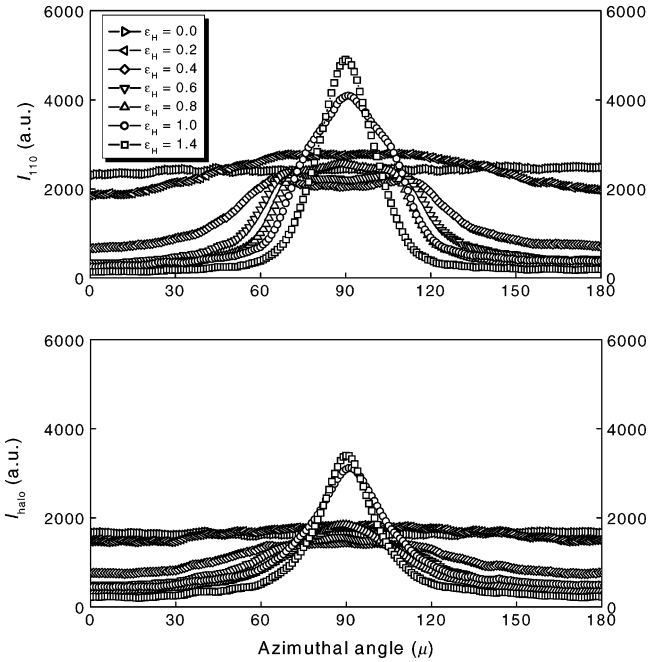

Figure 3. PEVA27: azimuthal intensity distribution of the 110 reflection (upper part) and of the amorphous halo (lower part), measured at the indicated imposed strains.

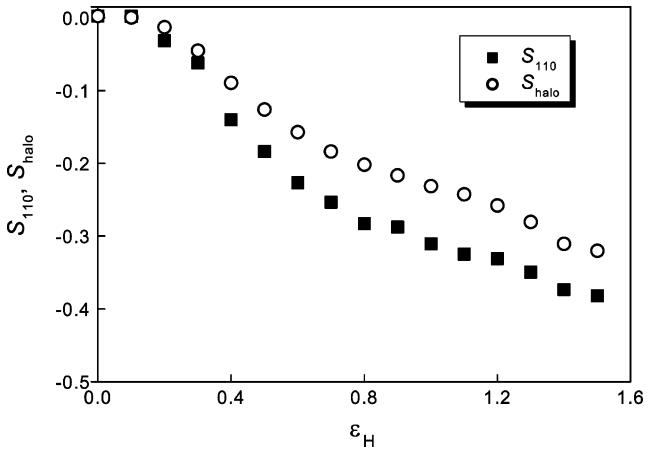

Figure 4. PEVA27: orientational order parameters associated with the 110 reflection and the amorphous halo as a function of the imposed strains.

polarizing microscope. Using a tilting compensator, we measured the optical path length differences Γ for the samples induced by the uniaxial stress. With the thickness of the measured sample the birefringence Δn was calculated for the different imposed strains. The results are presented in Figure 6.

The experimental birefringence includes two parts. One is produced by the oriented crystallites, and the other is induced by the stretched amorphous network chains. Following Taylor,[11] we treat the birefringence contributions of the amorphous phase, Δn_a, and of the crystalline phase, Δn_c, as additive. Then the total birefringence is

$$\Delta n = \phi_c \Delta n_c + (1 - \phi_c)\Delta n_a \tag{7}$$

where ϕ_c is the volume fraction of the crystalline material. A single crystal has a well defined birefringence, which we denote Δn_c°. The crystallites in semicrystalline materials are not uniformly oriented. Therefore, we have to ask about the

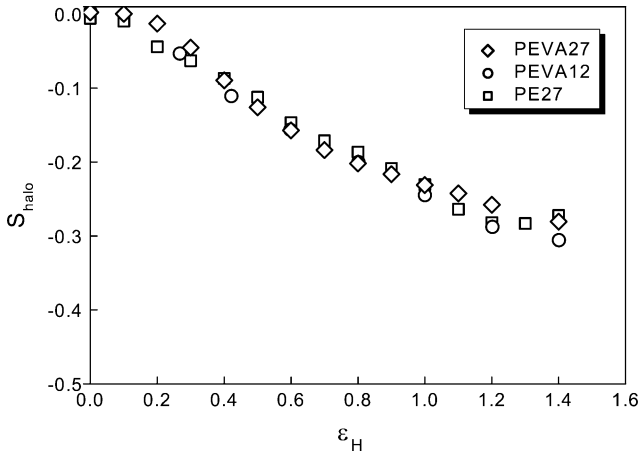

Figure 5. PEVA27, PEVA12, and PE27: variation of the orientational order parameter of the amorphous halo with the strain.

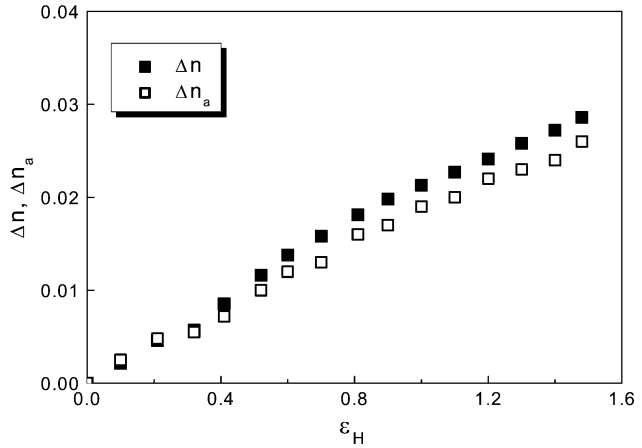

Figure 6. PEVA27: strain dependence of the sample birefringence Δn and of the birefringence Δn_a originating from the stretched amorphous chains.

birefringence produced by an aggregation of crystallites with a certain orientational distribution. Using Hermanns' order parameter, Stein derived the birefringence which results for a distribution of optically uniaxial crystals,[12] as being given by

$$\phi_c \Delta n_c = \phi_c \Delta n_c^\circ \frac{3\langle \cos^2 \delta \rangle_c - 1}{2} = \phi_c \Delta n_c^\circ S_c \tag{8}$$

δ is the angle between the crystalline chains and the stretching direction, and $\langle\ \rangle_c$ denotes an average over all crystallites. Hermanns' order parameter, S_c, characterizes the orientational order of the crystallites referring to the stretching direction. The birefringence Δn_c° of a single polyethylene crystal was set equal to the birefringence of crystals of the *n*-paraffin $C_{36}H_{74}$,[13] and the value is 0.0572.

We now can use the order parameter S_{110} derived from the X-ray scattering pattern for a determination of S_c and thus the birefringence of the crystal part. Applying an equation derived by Ogorodnik[14] to perform a transformation between orientational order parameters related to different sorts of lattice planes for uniaxially oriented samples, S_c and S_{hkl} can be related by

$$S_{hkl} = P_2(\gamma) S_c = \frac{3\langle \cos^2 \gamma \rangle - 1}{2} S_c \tag{9}$$

Here, γ is the angle between the normal vector of the *hkl* lattice plane and the chain direction. ($P_2(\gamma)$ is the second spherical harmonic.)

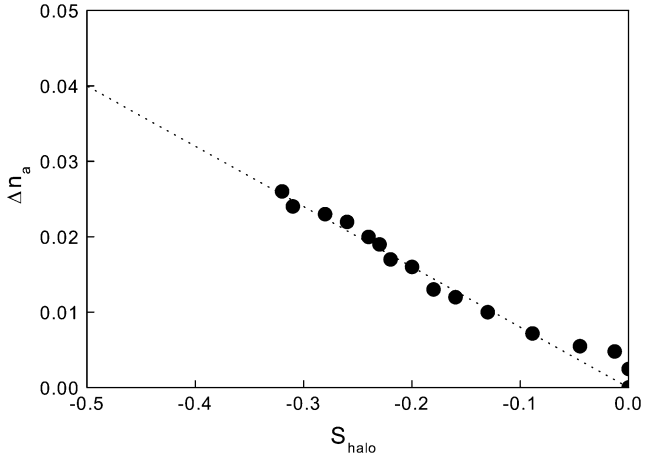

Figure 7. PEVA27: relationship between the birefringence of the stretched amorphous chains, Δn_a, and the orientational order parameter of the amorphous halo, S_{halo}.

Since the normal on the 110 lattice plane of a polyethylene crystal is perpendicular to the chain direction, we have

$$S_{110} = -0.5S_c \tag{10}$$

Combining eqs 8 and 10, inserting $\phi_c = 0.15$, the birefringence contribution from the crystals becomes

$$\phi_c \Delta n_c = -0.01716 S_{110} \tag{11}$$

Subtracting the crystal birefringence contribution from the experimentally obtained total birefringence, we obtained the birefringence Δn_a produced by the stretched amorphous network chains alone. The result is also presented in Figure 6.

Figure 7 compares Δn_a with the order parameter S_{halo} of the halo determined by WAXS. One finds a linear relation

$$\Delta n_a = 0.040 \frac{S_{halo}}{-0.5} \tag{12}$$

It indicates that for fully oriented amorphous chain sequences a limiting value

$$\Delta n_a^\circ = 0.040 \tag{13}$$

would be reached.

S_{halo} can be converted into the orientational order parameter of the amorphous chains

$$S_a = \frac{3\langle \cos^2 \delta \rangle_a - 1}{2} \tag{14}$$

($\langle\ \rangle_a$ now denotes an average in the amorphous regions only) by

$$S_{halo} = -0.5 S_a \tag{15}$$

using again eq 9. This leads to

$$\Delta n_a = \Delta n_a^\circ S_a \tag{16}$$

in analogy to eq 8.

3.3. Stress−Optical Law. For all polymer melts as well as stretched rubbers, the birefringence Δn is proportional to the tensile stress σ:[15,16]

$$\Delta n_a = C_{opt}\, \sigma \tag{17}$$

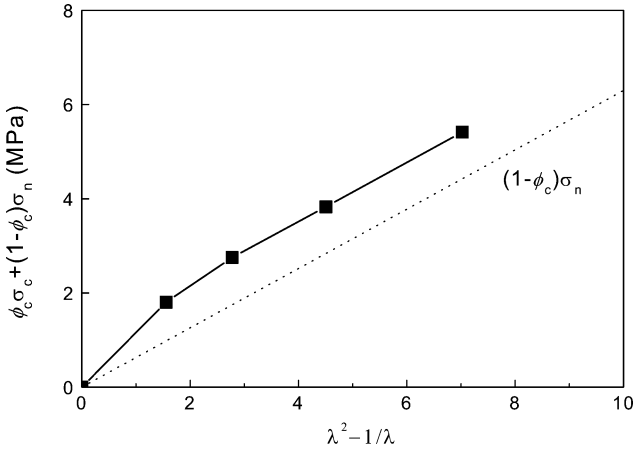

Figure 8. PEVA27: quasi-static stress−strain dependence presented in a plot of σ vs the rubber measure of strain $\lambda^2 - 1/\lambda$. The broken line represents the network stress $(1 - \phi_c)\sigma_n$.

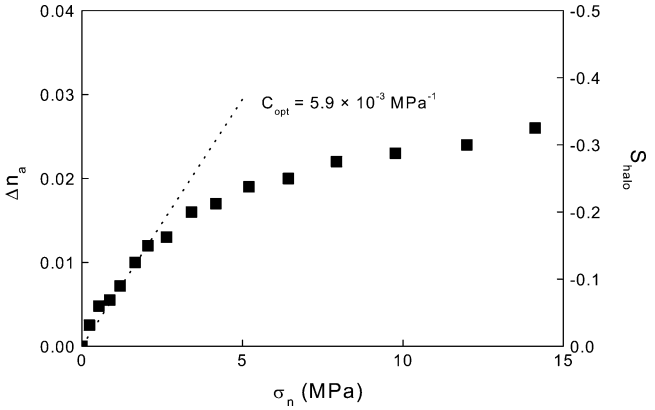

Figure 9. PEVA27: birefringence Δn_a and order parameter S_{halo} originating from the stretched amorphous chains as a function of the network stress σ_n. The slope of the broken line gives the stress−optical coefficient, $C_{opt} = 5.9 \times 10^{-3}$ MPa^{-1}.

Equation 17 is known as the "linear stress−optical rule".[17] The proportionality constant C_{opt} is called the "stress−optical coefficient", and its value describes a characteristic property of each polymer.

We measured the stress−strain curves of the sample and subtracted after stress relaxation measurements the viscous part σ_r. The result was the quasi-static stress $\phi_c\sigma_c + (1 - \phi_c)\sigma_n$. A separation into σ_c and σ_n was achieved by a plot of the quasi-static stress vs $\lambda^2 - 1/\lambda$, as suggested by Haward and Thackray.[18] Figure 8 presents the result. The dotted line which determines the stress at large strains is representative for a Gaussian network with a shear modulus of $G = 0.74$ MPa as given by the slope. With this modulus we calculated the dependence of the network stress on the strain ϵ_H. When ϵ_H is replaced by the birefringence Δn_a using the data in Figure 6, Figure 9 is obtained. The slope of the dotted line at the origin yields the stress−optical coefficient; the value is $C_{opt} = 5.9 \times 10^{-3}$ MPa^{-1}.

Obviously, the stress−optical law holds only for a limited range. Above $\sigma_n = 2$ MPa ($\lambda^2 - 1/\lambda \approx 3$, $\epsilon_H \approx 0.6$), the network stress σ_n deviates from the initial linear increase.

4. Discussion

In Figure 4 the amorphous orientation for all imposed strains seems to be somewhat lower than the orientation of the crystallites. However, this could be a wrong impression. Just consider that the halo is still expanded in meridional direction if the amorphous chains are perfectly oriented, which would

result in an experimental value S_{halo}, which is still above the limit -0.5. Hence, even if the intermolecular contribution is dominant for the amorphous halo, an intramolecular part always exists. An analysis led Pick et al.[4] to the equation

$$S_{halo} = \alpha(-0.5)S_a \tag{18}$$

where α is a factor with a constant value below unity. Therefore, the amorphous orientation under stress could well be comparable to the orientation of the crystallites.

This conclusion differs from that reached by Seguela et al.[19] based on birefringence measurements exclusively. They claimed that S_a is much smaller than the degree of orientation of the crystals. In fact, the derivation of S_a from birefringence measurements is problematic, due to the difficulty to obtain a reliable value for Δn_a°, the limiting value of the birefringence for a perfectly oriented, but still amorphous polyethylene sample. Firstly, the question of the chain conformation arises. Oriented chains in a melt occupy a straight tube whose cross section is 15% expanded compared to the crystallized state. Under such conditions chains are no longer in the all-trans state of the crystals but necessarily include a certain amount of kink defects. As was derived from the appearance of Raman spectra, this holds even for the hexagonal high-pressure phase of polyethylene, where the cross section of the tubes is intermediate between the crystalline and fluid state.[20] The presence of kink defects changes the local anisotropy and thus the birefringence. Secondly, and this presents an even more difficult problem, the birefringence of oriented polyethylene is strongly affected by the inner field. The polarizability tensor of the methylene group has a negative anisotropy, i.e., it has a smaller value in chain direction,[21] and the positive birefringence is caused by the positive anisotropy of the Lorentz tensor only.[22] Structure properties, i.e., density, crystallinity, orientation, gain under such conditions high relevance. As one surprising effect, an increase of the birefringence with decreasing density is theoretically predicted. This was used to explain that a sample of ultraoriented high-density polyethylene had a higher birefringence ($\Delta n = 0.063$[23]) than n-$C_{36}H_{74}$. Seguela et al. assumed in their evaluation of birefringence measurements a value $\Delta n_a^\circ = 0.2$, which is about 4 times as large as Δn_c°. Our combination of birefringence measurements with an X-ray determination of the orientational order parameter shows, however, that this cannot be true. The limiting value of Δn_a reached for a perfect orientation is 0.04 (or even smaller, when taking into account $\alpha < 1$). We have presently no theoretical explanation for this value, but the stretching of the amorphous chains in the sample is obvious. The linear relationship between Δn_a and S_{halo} shown in Figure 7 indicates that both properties are proportional to S_a and S_{halo} according to eq 18 and Δn_a following eq 16.

The limitation of the stress−optical law to the range of lower strains is not surprising. The birefringence will always saturate, while the stress continues to increase. The behavior is well-known from the literature. Treloar[24] showed that only below $\epsilon_H = 1.4$ ($\lambda^2 - 1/\lambda = 16$) the chains of a rubber are not yet stretched tightly, so that chains can show the Gaussian properties. Also, Janeschitz-Kriegel[15] pointed out that the coefficient C_{opt} is only constant up to a tensile stress on the order of 1 MPa. Matsumoto and Bogue[25] studied the stress birefringence for a uniaxially elongated rubberlike polystyrene. They again found that for stresses above 1 MPa the linear relationship between the stress and the birefringence ends.

Acknowledgment. Support of this work by the Deutsche Forschungsgemeinschaft (Sonderforschungsbereich 428) is gratefully acknowledged. Thanks are also due to the "Fonds der Chemischen Industrie" for financial help. We greatly appreciate the advice in the measurements of birefringence given by Dr. Werner Stille.

References and Notes

(1) Hiss, R.; Hobeika, S.; Lynn, C.; Strobl, G. *Macromolecules* **1999**, *32*, 4390.
(2) Hobeika, S.; Men, Y.; Strobl, G. *Macromolecules* **2000**, *33*, 1827.
(3) Hong, K.; Rastogi, A.; Strobl, G. *Macromolecules* **2004**, *37*, 10165.
(4) Pick, M.; Lovell, R.; Windel, A. *Polymer* **1980**, *21*, 1017.
(5) Keller, A. *J. Polym. Sci.* **1955**, *15*, 31.
(6) Hermanns, P.; Platzek, P. *Kolloid Z.* **1939**, *88*, 68.
(7) Polanyi, M. *Z. Phys.* **1921**, *7*, 149.
(8) Monar, K.; Hebenschuss, A. *J. Polym. Sci., Part B: Polym. Phys.* **1999**, *37*, 3401.
(9) Murthy, N.; Minor, H.; Bednarczyk, C.; Krimm, S. *Macromolecules* **1993**, *26*, 1712.
(10) Simanke, A.; Alamo, R.; Galland, G.; Mauler, R. *Macromolecules* **2001**, *34*, 6959.
(11) Taylor, G.; Darin, S. *J. Appl. Phys.* **1955**, *26*, 1075.
(12) Stein, R.; Norris, F. *J. Polym. Sci.* **1956**, *21*, 381.
(13) Bunn, C.; deDaubeny, R. *Trans. Faraday Soc.* **1954**, *50*, 1173.
(14) Ogorodnik, K. *Sov. Phys. Crystallogr.* **1978**, *23*, 557.
(15) Janeschitz-Kriegel, H. *Polymer Melt Rheology and Flow Birefringence*; Springer: Berlin, 1983; p 62.
(16) Treloar, L. *The Physics of Rubber Elasticity*; Clarendon Press: Oxford, 1975; p 180.
(17) Strobl, G. *The Physics of Polymers*; Springer: Berlin, 1996; p 338.
(18) Haward, R.; Thackray, G. *Proc. R. Soc. London, A* **1968**, *302*, 453.
(19) Seguela, R.; Rietsch, F. *J. Mater. Sci., Lett.* **1990**, *9*, 46.
(20) Eckel, R.; Schwickert, H.; Buback, M.; Strobl, G. *Polym. Bull.* **1982**, *6*, 559.
(21) Pietralla, M. *J. Polym. Sci., Polym. Phys. Ed.* **1980**, *18*, 1717.
(22) Pietralla, M.; Grossmann, H.-P.; Krger, J. *J. Polym. Sci., Polym. Phys.* **1982**, *20*, 1193.
(23) Mead, W.; Desper, C.; Roger Porter, S. *J. Polym. Sci., Polym. Phys. Ed.* **1979**, *17*, 859.
(24) Treloar, L. *The Physics of Rubber Elasticity*; Clarendon Press: Oxford, 1975; p 87.
(25) Matsumoto, T.; Bogue, D. *J. Polym. Sci., Polym. Phys. Ed.* **1977**, *15*, 1663.

MA051726O